Effect of trapped wire-rope debris upon an EM instrument's LMA chart-trace

Lorant B. Geller, and Gilles Rousseau

MRL 90-008 (TR) February, 1990

EFFECT OF TRAPPED WIRE-ROPE DEBRIS UPON AN EM INSTRUMENT'S LMA CHART-TRACE

by

Lorant B. Geller*, and Gilles Rousseau**

ABSTRACT

A contracted project was undertaken by CANMET in July, 1988. Its objective was to comparatively evaluate the performance of a range of commercially available electro-magnetic (EM) wire-rope test instruments.

As part of this project, test-ropes were specially designed and manufactured by Wire Rope Industries Ltd. of Pointe Claire, Que. These included $1\frac{3}{4}$ in., 6×27 flattened strand constructions with artificial defects. The latter involved sections where the fibre-core was replaced by plastic tubes, filled with various types of powdered materials.

In this report the authors describe the tests undertaken, and the results achieved, to demonstrate that the loss-of-metallic-area (LMA) chart traces of the EM instruments are not — or at any rate very little — affected by the presence of trapped magnetic debris in the wire-ropes.

---

* Research Scientist, Mining Research Laboratories, CANMET, and ** Physical Scientist, Metals Technology Laboratories, CANMET, Energy Mines and Resources Canada, Ottawa.

Keywords: Wire-rope-debris; Non-destructive-testing; EM instruments.

EFFET DES DEBRIS DE CABLE D'ACIER PIEGES
SUR LE TRACE D'UNE COURBE DE PSM D'UN INSTRUMENT EM

Lorant B. Geller* et Gilles Rousseau**

RÉSUMÉ

Un contrat a été réalisé par CANMET en juillet 1988. L'objectif était de comparer les rendements de divers instruments électromagnétiques (EM) pour essais au câble d'acier, disponibles dans le commerce.

Dans le cadre du contrat, des câbles d'essai spéciaux ont été conçus et fabriqués par Wire Rope Industries Ltée de Pointe-Claire au Québec, notamment des câbles de 1,75 po composés de 6x27 brins plats comportant des défauts artificiels. Ces derniers présentaient des sections dont l'âme en fibres était remplcée par des tubes de plastique remplis de diverses matières en poudre.

Dans le présent rapport, les auteurs décrivent les essais effectués et les résultats obtenus pour démontrer que les tracés des courbes de perte de surface métallique (PSM) des instruments EM ne sont pas, ou du moins sont très peu, modifiés par la présence de débris magnétiques piégés dans les câbles d'acier.

*Chercheur scientifique, Laboratoires de recherche minière, CANMET, et
**chercheur en sciences physiques, Laboratoire de la technologie des métaux, CANMET, Energie, Mines et Ressources Canada, Ottawa.

CONTENTS

TABLES

FIGURES

INTRODUCTION

DC electro-magnetic (EM) instruments used for wire-rope testing consist of a magnetic circuit, made-up of permanent magnets and of an iron yoke, with the magnetic flux circuit being closed by the length of wire-rope that is being inspected. The mean metallic area of the rope is evaluated by measuring the magnetic flux flowing in this circuit. Field strength can either be measured at the yoke-pole with Hall effect sensors, or directly in the rope, with an encircling coil. Basically, the instrument correlates the field strength to an equivalent magnetic area, which is assumed to be proportional to the rope's metallic cross-section.

Magnetic-flux measurements are intended to detect the wire-rope's loss of metallic area (LMA), brought about by wear and corrosion. Rope deterioration produces, inter alia, corrosion products and wear debris, some of it in the form of fine powder trapped inside the rope. Since these materials are ferromagnetic, they can drive a small part of the magnetic field, thus slightly contributing to the total field. This additional field can, in theory, result in an overestimation of the true metallic cross-section of the rope. According to some authors the trapped magnetic debris can be responsible for errors, possibly partial or even major, during LMA measurements with EM instruments. With our work we wish to quantify the level of these errors.

Magnetization of a length of rope is nearly uniform if each individual wire in the rope has a constant cross-section along the length of the sensor-head, and if the applied magnetic field is strong enough to magnetically saturate each wire. In this case a straightforward correlation can be obtained between magnetic induction and the metallic rope cross-section. This follows as a consequence of the ease with which an elongated body, such as a wire, can be magnetized. For a short object, however, magnetic saturation is not so easy to achieve. This is due to the presence of a demagnetizing effect. Magnetization of a ferromagnetic body of finite length produces magnetic free poles on the surface, where the normal component of the magnetization changes ($\mathbf{n}.\mathbf{M}\neq 0$)*. The induced field is known as the demagnetizing field Hd, because it always tends to oppose the applied field **H**. Hence, the effective field acting on the metallic body is always less than the applied field (1, 2). Hd is proportional to the magnetization change, and inversely proportional to the distance between the poles (or to the length of the object).

---

* for definition of symbols see List of Symbols section

The practical significance of the demagnetizing field is evident when noting the considerable strength of the applied magnetic fields that are needed in order to saturate short ferromagnetic objects. Consider, for example, a spherical iron specimen: the applied field must exceed 7,120 Oersted (Oe) in order to bring it to saturation, while an infinitely long iron wire would require only 10 Oe.

If the abovenoted demagnetizing factor is taken into account, it can be assumed that the magnetic field produced and carried by a loose powder — that is made up of fine particles trapped inside a wire-rope — will be very low. This is so because each particle can be considered as a spherical specimen, surrounded by a constant magnetic field. This assumption is valid if each particle is not in direct physical contact with the rest of the ferromagnetic body. Also, it is a fair assumption that while the magnetic field produced by the EM tester is strong enough to saturate a length of the wire rope, it does not strongly interact with the trapped debris. It follows that the total magnetic induction flowing in the magnetic circuit is not greatly affected by the debris trapped inside the wire-rope.

We experimentally investigated the effect of the wire-rope- debris in two different ways:

(1) by magnetic property measurement of the rope-debris itself, and

(2) by measuring the effect upon the EM instrument's LMA chart-trace of the debris trapped inside the wire-rope.

MAGNETIC PROPERTY MEASUREMENTS

We undertook laboratory measurements in order: (a) to characterize the level of magnetization of the trapped debris at magnetic rope-saturation conditions, and (b) to compare these values with magnetization data of selected materials. The magnetic behaviour of the trapped materials was obtained by plotting their hysteresis curve with an electromagnet hysteresisgraph (LDJ model 3500).

Normally, in order to plot a hysteresis curve, the sample must have the shape of a toroid. But since in our case the materials are in powdered form, it is much simpler to fabricate cylindrical specimens instead, and then to measure their magnetic properties with an electromagnet (Fig. 1). Such specimens were fabricated by filling a steel mould with a mixture of powder and epoxy, and by then compressing this mixture with a hydraulically actuated piston. Excess epoxy was removed by a multilayer screen assembly. Figure 1 shows the sample fabrication process. Approximate specimen dimensions are: 1.5 cm diameter×0.85 cm length.

For purposes of comparative reference we selected the following materials:

(a) Steel rod: used as a reference material for the continuous medium. Its saturation magnetization is around 18,000 Gauss;

(b) Iron powder: on comparing this material with the solid steel rod, we can observe the demagnetizing effect that acts on each particle. Intrinsic magnetic material properties are, however, similar to those of the steel rod. Two types of iron powder were used: the MP-41 and the electrolytic iron (Table 2);

(c) Ferrous oxide powder: this material, known also as magnetite or ferrite, contains mainly magnetic ferrous oxide Fe_3O_4 ($Fe_2O_3.FeO$); it has intrinsic magnetic properties similar to the magnetic iron oxide debris. It is commercially available as E-96 magnetite;

(d) Wire-rope corrosion products: this material was obtained by us from the surface of one of the discarded operational wire-ropes (our rope #7) during shop-floor testing. The base material is slightly magnetic. It was ground into a fine powder before being tested.

The material and dimensions of the cylindrical test specimens are listed in Table 1.

After fabrication of the cylindrical samples, the hysteresis curves were plotted for each material. The loops thus obtained are, in fact, not the intrinsic hysteresis curves of the materials, because of the demagnetizing effect that is present. Two demagnetizing effects must be considered:

(1) the effect associated with the geometry of the samples. This geometric effect acts on the cylindrical sample. It is quite small for the cemented powdered specimens, because dM/dX is close to zero at the pole-to-sample interface. Even so, however, this effect is clearly in evidence in case of the solid steel rod specimen, by shifting the hysteresis curve over to the right;

(2) the effect associated with the consistency of the samples. It arises only in case of powdered materials. It is related to the morphology, i.e., to the shape and density, of the powder.

Both demagnetizing effects have an influence upon the magnetic fields that are needed to saturate the samples; however, they do not alter the level of saturation-magnetization. Furthermore, it should be noted that: (a) the hysteresis curves plotted with our cemented powder samples do, in fact, closely resemble the real-life behaviour

of similar powders trapped inside mine-shaft wire-ropes, and (b) that the two materials (i.e., the cemented and the powder core) also have the same densities. Figures 3 to 7 illustrate our test results. In Table 2 we list the magnetization-data of the powdered samples, as measured inside a field of 1,000 Oe, with a volumetric filling-factor of about 55%.

The data in Table 2 provide all pertinent information associated with the problems caused by trapped rope-debris. As expected, a solid ferrous medium is easy to magnetize to saturation. While it is difficult to calculate the demagnetizing factor acting on the rod, the hysteresis loop indicates that with a magnetic field of 300 Oe one can obtain magnetic saturation of the steel, which is usually around the level of 18,000 Gauss (Ms). Without the geometric effect mentioned, some 20 Oe might be enough to achieve the same effect.

In case of the four other powdered samples, the geometric demagnetizing effect is of less significance, because the level of saturation-magnetization is less for these materials. The latter quantity is a function of the samples' volumetric filling-factor and of the intrinsic saturation-magnetization level of the materials. For the iron-powder samples the Ms should be around 9,000 Gauss, and for the ferrite-sample it should be about 2,500 Gauss. The results in Table 2 are in good agreement with these values. However, due to the demagnetizing effect it is difficult to state when the sample will reach saturation.

An important aspect that can be observed as a result of our measurements is the value obtained for the saturation-magnetization of the rope debris. The latter is a mixture of wear-particles, corrosion products, and of rope-lubricants; its Ms is only half of the equivalent value for the ferrite materials. At 1 Kilo-Oe, the magnetization of the corrosion products is only 8.5% that of the steel specimen (Table 2). Consequently, the effect of rope-debris on the EM instrument's chart-trace magnitude should be, at most, $\frac{1}{10}$-th that of the solid iron.

MEASUREMENT OF THE EFFECT OF TRAPPED WIRE-ROPE DEBRIS UPON THE LMA CHART-TRACE

(1) Background

In early 1989 two stranded test-ropes were fabricated by Wire Rope Industries Ltd. for CANMET's contracted project (3, 4, 5). The ropes are of $1\frac{3}{4}$ in. 6×27, flattened strand construction. A sketch of the cross-section of these ropes is shown in Figure 8. Each rope contains artificial defects, intentionally introduced during the

manufacturing process. The first type of defect is a reduction in the ropes' metallic cross-sectional area, obtained by replacing some of the wires by smaller ones. The length of the "defective" area is 6 ft, and the theoretical LMA is between 7.0% and 7.5%. The second type of defect was obtained by replacing the nylon rope core along 3 ft and 6 ft lengths with plastic tubes, filled with the various powders discussed in the previous report section. A third type of defect was introduced into the test-ropes during their closing process: at this stage some of the welds broke where the larger and smaller diameter wires were joined together. The manufacturer reported the number of broken wires to the best of his ability. It was, however, impossible to be certain as to the exact number, and location, of all the breaks that occurred unintentionally. Most of these breaks are assumed to have occurred at the extremities of the major LMA zones. Tables 3 and 4 summarize the defect-locations, as reported by the rope manufacturer. Figures 9 and 10 are a sketch of what should, in theory, be seen on the LMA chart-traces, provided the instruments correctly quantify these defective rope areas.

We now pose the important question as to what might be the magnitude of the signal that the LMA sensor will pick up, if the magnetic core is brought to saturation? The plastic tube used for core replacement is 6 ft long, with a $\frac{3}{4}$ in O.D. and a $\frac{5}{8}$ in. I.D. It is filled with the various magnetic powders described earlier in this report. The equivalent magnetic steel area is, therefore:

$$\%\text{Equivalent Magnetic Area} = Ac/Ar \times Mp/Ms \times 100\% \quad \text{——} \quad \text{Eq. 1}$$

where,

Ac — the rope's core area = 1.979 cm^2;

Ar — the rope's metallic cross-sectional area = 8.903 cm^2;

Mp — magnetization at saturation of the powder (Table 2);

Ms — magnetization at saturation of the steel = 18,000 Gauss.

Since the EM tester measures the magnetic flux's cross-sectional area, Equation 1 directly gives the LMA output of such an EM instrument. Calculating the error caused by the powder filled core, we obtain the values listed in Table 5.

The theoretical effect of the magnetic core is illustrated in Figures 9 and 10 by the rise of the LMA signals; the latter's magnitude is proportional to the value obtained from Equation 1.

(2) Results of shop-floor testing

The two test ropes were inspected with four EM testers, namely with the:

(1) Canadian Magnograph,

(2) Canadian Rotescograph,

(3) American LMA-250 instrument, and the

(4) German tester, designed by the WBK organization.

For the loose filler materials in the rope-cores (see Tables 3 and 4) all EM testers produced similar outputs on their chart traces (no results have been received to date for the German instrument). Figures 11 and 12 are copies of the relevant sections of the Rotescograph LMA chart traces, i.e., of those sections that contain the artificial defects of interest. It is important to note that in order to obtain a picture as to where in the rope the various artificial defects are located, the LMA and LF (Local Fault) traces must be considered in conjunction.

For both test-ropes A and B the iron powder filler produces a signal output on the LMA chart trace of some 1.0%–1.6%. The magnetite's LMA signal is in the order of about 0.5%. The corrosion-product signals, however, can hardly be detected, if at all, on either the LMA or the LF chart trace. These LMA signal-amplitudes are listed in Table 6. We wish to stress that in this report we are only concerned with the signals due to the "trapped debris", i.e., to the various loose fillers in the rope-core. A detailed review of the entire chart lengths of all the EM instruments is given elsewhere (6).

On comparing the actually measured LMA values (Table 6) with the theoretical values (Table 5), one notes that the powder filler materials hardly show up. Consider, for example, the iron powder filler: its cross-sectional area represents a 22% increase in the rope's metallic cross sectional area (with a 55% filling-factor). Were the iron-powder brought up to saturation magnetization levels, the LMA trace should record a rise of some 11%. However, the EM testers only recorded a maximum signal change of 1.6%, which is about $\frac{1}{10}$-th of the theoretical value.

For the other two powdered core-materials, the signals picked up are actually close to the resolution limit of the chart recorder's gain-setting. Especially in case of the corrosion products (i.e., the rope debris), it is difficult to distinguish them from the background noise, even though their cross-sectional area represents a change of more than 20% in the rope's total metallic cross-sectional area.

It is obvious, therefore, that trapped oxide and wear debris can not cause significant errors in the LMA channel chart traces, because it requires a huge amount of debris to produce a signal strength that will produce a 1.0% LMA trace change.

The results illustrated in Figures 9 and 11 suggest that the location of the powder filled cores might not have been accurately mapped: the length of the powder filled cores, and their locations in test rope A, are not unequivocally reflected in the EM tester's output.

CONCLUSIONS

It has been shown that the rope debris is only weakly ferromagnetic, and that the debris trapped in a wire-rope can not produce a significant error in the EM tester's LMA channel chart trace. We arrived at this conclusion because: (a) of the small intrinsic saturation-magnetization of the compound removed from the discarded operational rope in question, (b) effective magnetization of the trapped powder (i.e., of the debris) needs a very high magnetic field, due to the demagnetizing effect acting on each particle, and (c) only a fraction of the total debris is trapped inside the wire-rope; the remainder is scraped off, or otherwise removed during normal operating conditions.

Others have arrived at the same conclusion. As an example, Kitzinger and Naud (7) found that with magnetite tightly packed inside a 16 in. long and 0.375 in. I.D. plastic tube, the output of the loss-of-metallic area sensor of their instrument (i.e., of the Magnograph) was less than 3.0% that of a steel rod of the same size. If hematite replaced the magnetite, there was no measurable output. Others (8) examined the LF signals of a range of EM instruments with a number of ropes, including a 42 mm, 1 × 164 full-locked-coil construction with many artificial defects. The latter included filed cavities filled: (a) with magnetic corrosion products, and (b) with non-magnetic corrosion products. The non-magnetic products were located at rope-fault numbers 1, 11, 25, and 26; the magnetic ones at rope-fault numbers 2, 4, 18, and 24. The chart-traces showed little, if any, difference for the two. We reproduce three charts (numbers 2.1.2, 2.2.2, and 2.3.2), as obtained with the German WBK instrument (Figures 13, 14, and 15 to 15b).

Even so, though, one often hears about contrary opinions. In this case it is claimed that trapped debris is the cause of serious mistakes in estimating a wire-rope's loss-of-breaking-strength (LBS), because it is said to show up on the EM instrument's LMA chart as if it were a solid metal section without, however, any strength to it.

Rope debris might, perhaps, cause another type of measuring error. This could, conceivably, occur if the debris accumulates along the instrument's magnetic path, e.g.,

by clinging to the magnetic poles. Should this happen, the reluctance of the circuit will be decreased, and the LMA signal will slowly drift, as the debris accumulates. Therefore, the sensor-head design should take account of this possible difficulty.

REFERENCES

1. Bozorth, R.M. "Ferromagnetism"; Van Nostrand Cie, N.Y., p. 845; 1951.

2. Chen, C.H. "Magnetism and metallurgy of soft magnetic materials"; Dover Publ. Co., p. 534; 1986.

3. Geller, L.B.; Udd, J.E.; and Mitchell, E.W. "Comparative evaluation of mine-shaft wire-rope NDT instruments: a search for, and analysis of, background information — contribution to the Canada/USBM/Ontario MOL joint R&D program"; CANMET Division Report MRL 88-78, 139 pp; July 1988.

4. Geller, L.B.; Anderson, G.L.; Miscoe, A.J.; and Mitchell, E.W. "The safety of mine-shaft wire-ropes — cooperative work by Canada and the U.S.A."; CANMET Division Report MRL 89-14, 28 pp; February 1989.

5. Geller, L.B.; Udd, J.E.; Blanchard, R.; and Daniel, K.E. "About electro-magnetic wire-rope testing in New Brunswick mines, and related data"; CANMET Division Report MRL 89-40, 51 pp; October 1989.

6. Geller, L.B.; Rousseau, G.; Poffenroth, D. "Canada/NB MDA project on mine-shaft rope testing; stranded ropes with artificial defects"; CANMET Division Report MRL 90-15, 30 pp; February 1990.

7. Kitzinger, F.; and Naud, J.R. "New developments in electro-magnetic testing of wire rope"; CIM Bulletin, pp 99-104; June 1979.

8. Commission of European Communities, Directorate General (V), Mines Safety and Health Commission; "Non destructive testing of wire ropes; tests on the performance of seven instruments mainly on locked coil mine hoisting ropes"; SMRE, Research and Laboratory Services Division, Health and Safety Executive, UK, 177 pp; 1978 (confidential).

LIST OF SYMBOLS

Symbol:	Definition:	Units:
B	Magnetic induction, or simply induction	Gauss
Bm	Maximum induction	Gauss
Bms	Level of saturation induction of steel	Gauss
Br	Remanence	Gauss
BoHo	Maximum energy product	Gauss-Oersted
d/dx	Spatial first order derivative operator	
H	Applied magnetic field	Oersted (Oe)
Hd	Demagnetizing field	Oe
Hc	Coercive force	Oe
Hm	Maximum applied magnetic field	Oe
L-AREA	Hysteresis losses	Gauss-Oe
M	Magnetization	Gauss
Ms	Saturation magnetization	Gauss
Mu	Permeability	
n	Unity vector normal to surface	

Note: symbols in bold face are vectorial quantities

APPENDIX

Tables 1, 2, 3, 4, 5, and 6

as well as Figures 1 to 15b, inclusive

Sample	Powder	Dia cm	Length cm	Relative density %
Solid steel rod	no	1,29	1,59	100
Electrolytic iron	yes	1,50	1,84	57
MP41 (iron)	yes	"	0,85	53
E96 (magnetite)	yes	"	0,85	-
Rope debris	yes	1,60	1,04	-

Table 1 — Samples used for magnetic measurements

Sample	Hm oersted	Bm Gauss	Bm/Bms %
Solid steel rod	300	17500	100
Electrolytic iron	1000	8590	50
MP41	1000	7804	45
E96	1000	2183	13
Rope debris	1000	1462	8.5

Table 2 — Measurement of maximum induction values

Location ft	defect(s)
0-24	no defects
at 24	1 broken outer wire
30-36	7.02%LMA (outer)
at 36	1 broken outer wire
at 42	1 broken outer wire
42-48	7,57%LMA (outer)
at 48	4 broken outers & 2 broken inners
at 54	1 broken outers & 3 broken inners
54-57	7,04%LMA (inner) & magnetite for core
57-60	7,04%LMA (inner)
63-66	iron powder for core
at 66	1 broken inner wire
66-69	7,54%LMA (inner) & iron powder for core
69-72	7,54%LMA (inner)
at 72	1 broken inner wire
75-81	used rope rust for core

Table 3 — Rope manufacturer's mapping of defects in test-rope A

location ft	defect(s)
0-24	no defects
at 24	2 broken outer wires
30-36	7,02%LMA (outer wires)
at 36	2 broken outer wires
at 42	3 broken outer wires
42-48	7.57% LMA (outer wires)
at 48	5 broken outers & 2 broken inners
at 54	2 broken inner wires
54-60	7.04% LMA (inner wires)
at 60	4 broken outers & unknown inners
66-69	7.54%LMA (inner wires)
69-72	7.54%LMA & magnetite powder for core
at 72	4 broken inner wires
78-84	iron powder for core
90-96	used rope rust for core

Table 4 — Rope manufacturer's mapping of defects in test-rope B

Filler	%LMA
Iron	1.1
Magnetite	3
Rope debris	2

Table 5 — Theoretical %LMA values, due to powder-filled rope cores

Filler	rope A*	rope B
Iron	1,0	1,6
Magnetite	0,4	0,5
Rope debris	0,2	0,3

*: Location of core fillers is uncertain for rope A

Table 6 — Maximum Rotescograph %LMA values, due to powder-filled rope cores

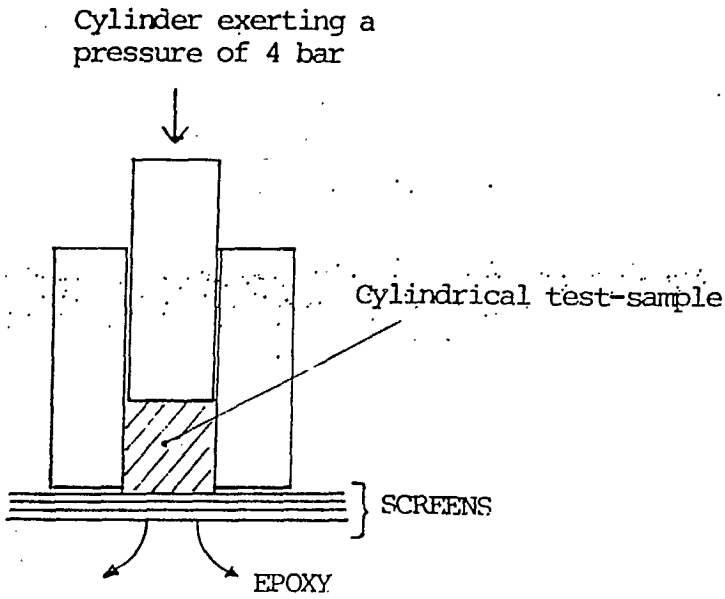

Fig. 1 — Fabrication of cylindrical test-samples

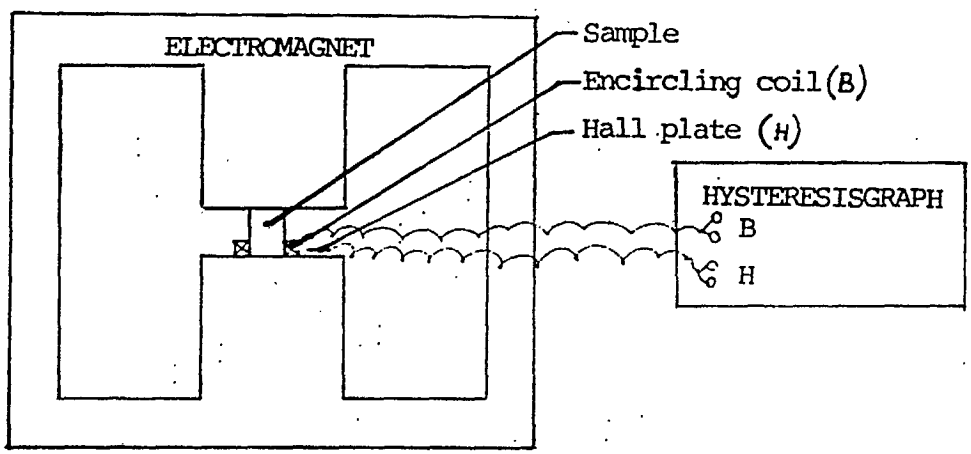

Fig. 2 — Set-up to measure magnetic properties of powdered materials

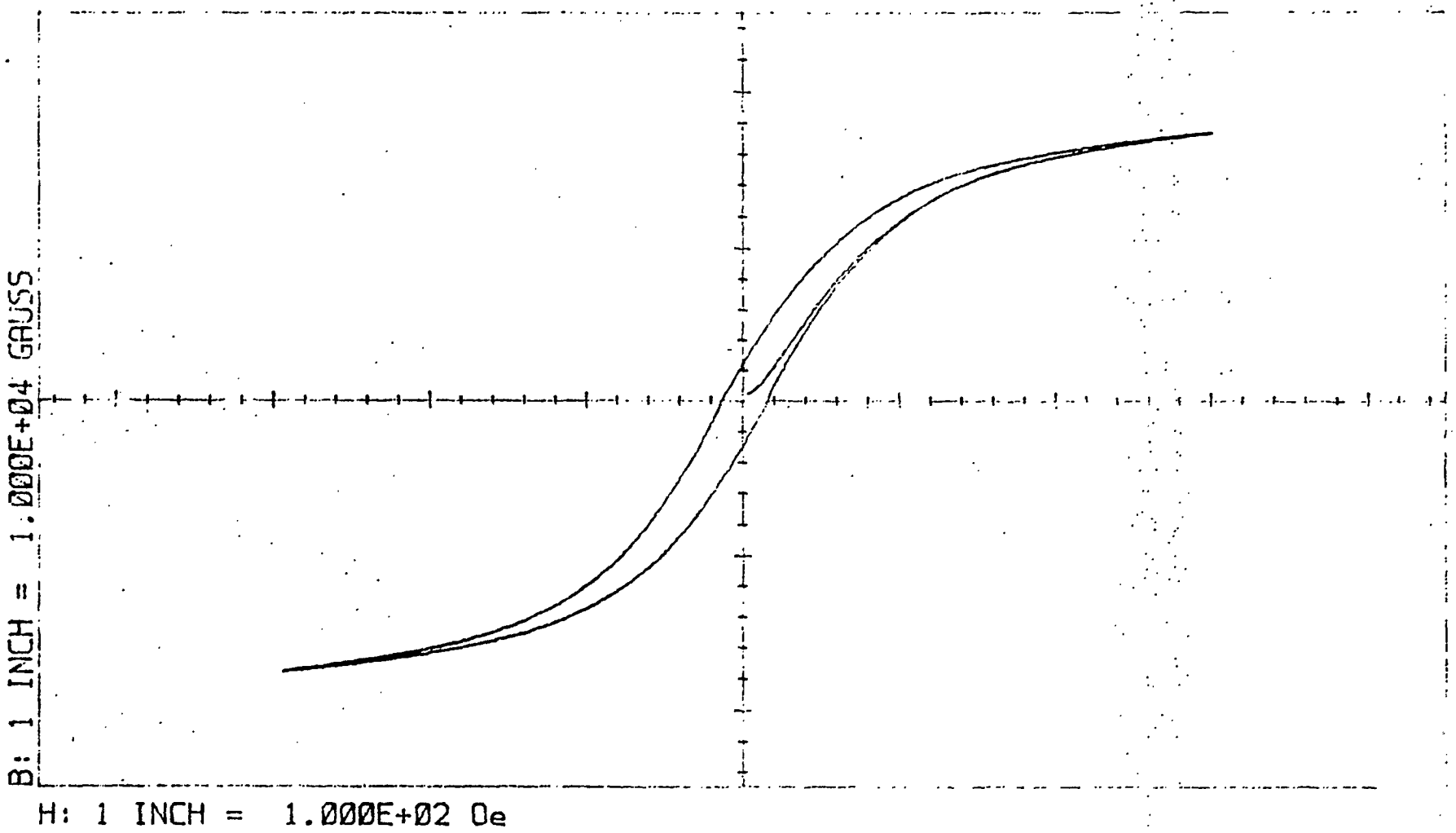

Solid steel specimen

Hm= 2.973E+02 Oe
Bm= 1.753E+04 GAUSS
Hc = 1.425E+01 Oe
Br= 2.672E+03 GAUSS

BoHo= 8.667E+03 GAUSS-Oe
Ho= 5.500E+00 Oe
Bo= 1.576E+03 GAUSS
L-AREA= 8.382E+05 G-Oe
Mu @ Bm= 5.895E+01

Fig. 3 — Hysteresis loop of solid steel specimen

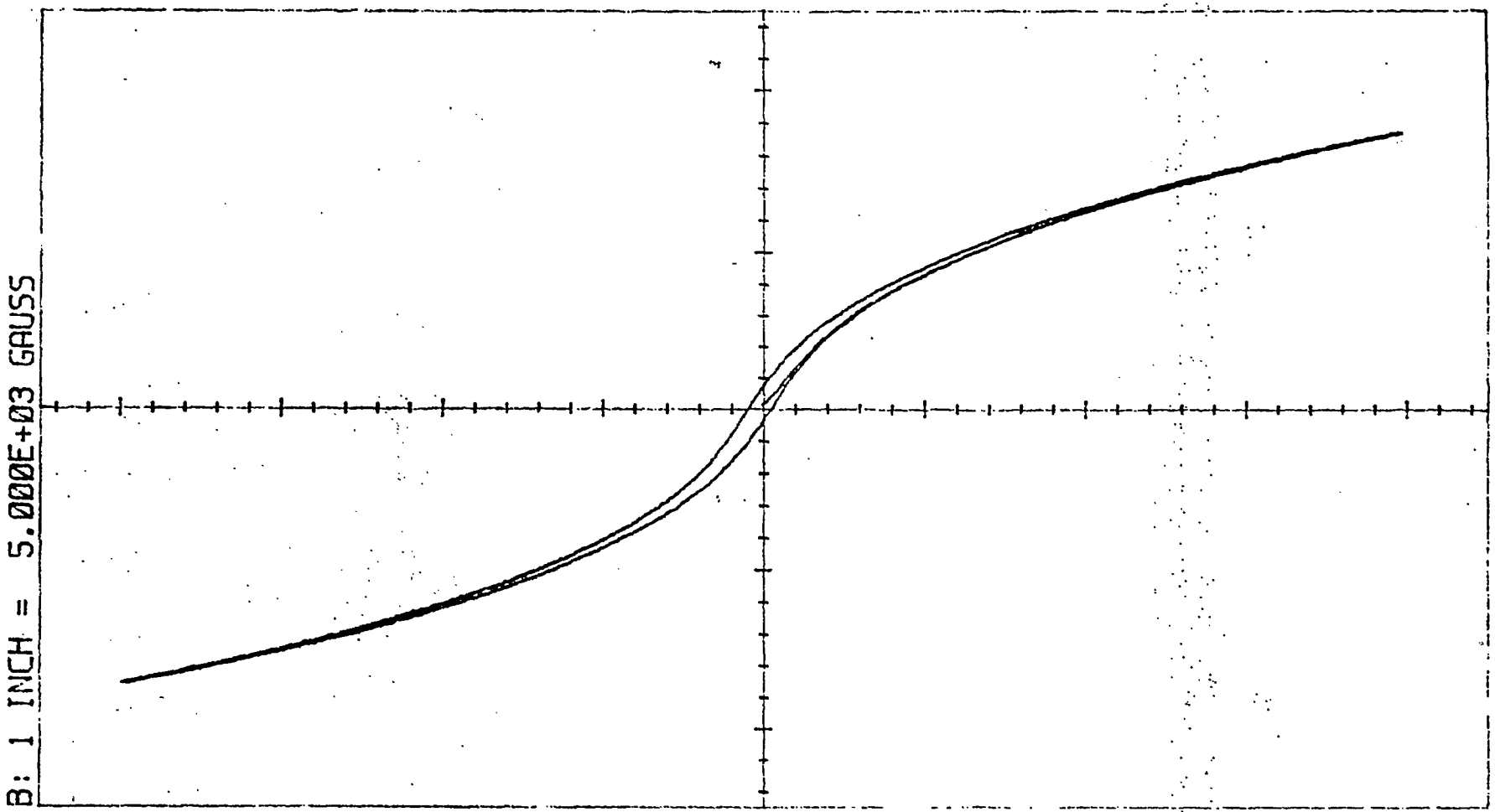

Electrolytic iron powder

Hm= 9.985E+02 Oe
Bm= 8.587E+03 GAUSS
Hc= 1.875E+01 Oe
Br= 5.565E+02 GAUSS

BoHo= 2.565E+03 GAUSS-Oe
Ho= 8.500E+00 Oe
Bo= 3.018E+02 GAUSS
L-AREA= 4.199E+05 G-Oe
Mu @ Bm= 8.600E+00

Fig. 4 — Hysteresis loop of electrolytic iron-powder specimen

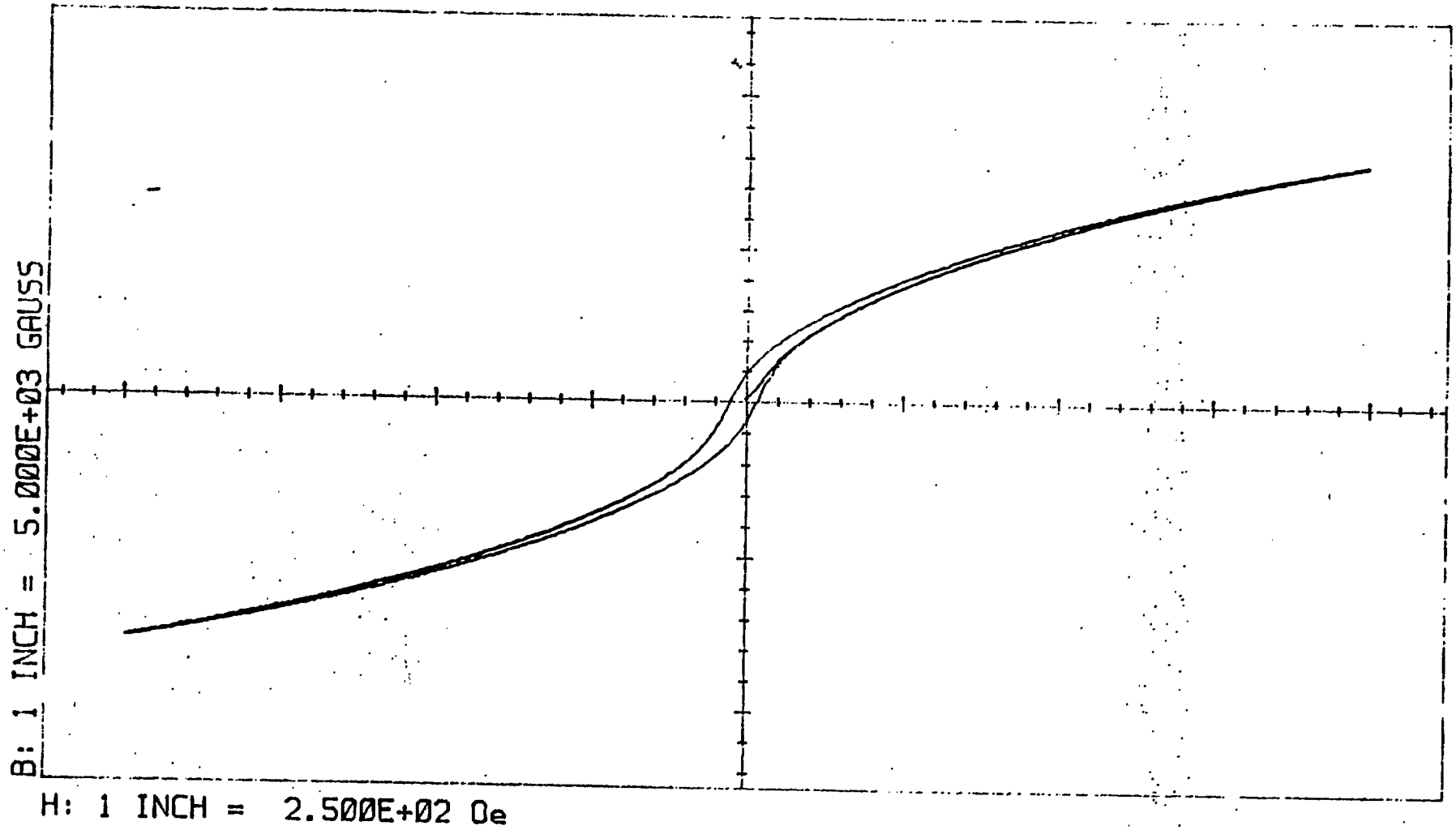

MP41 POWDER
Hm= 9.983E+02 Oe
Bm= 7.804E+03 GAUSS
Hc= 2.150E+01 Oe
Br= 7.592E+02 GAUSS

BoHo= 3.928E+03 GAUSS-Oe
Ho= 8.500E+00 Oe
Bo= 4.621E+02 GAUSS
L-AREA= 4.277E+05 G-Oe
Mu @ Bm= 7.818E+00

Fig. 5 — Hysteresis loop of MP-41 powder specimen

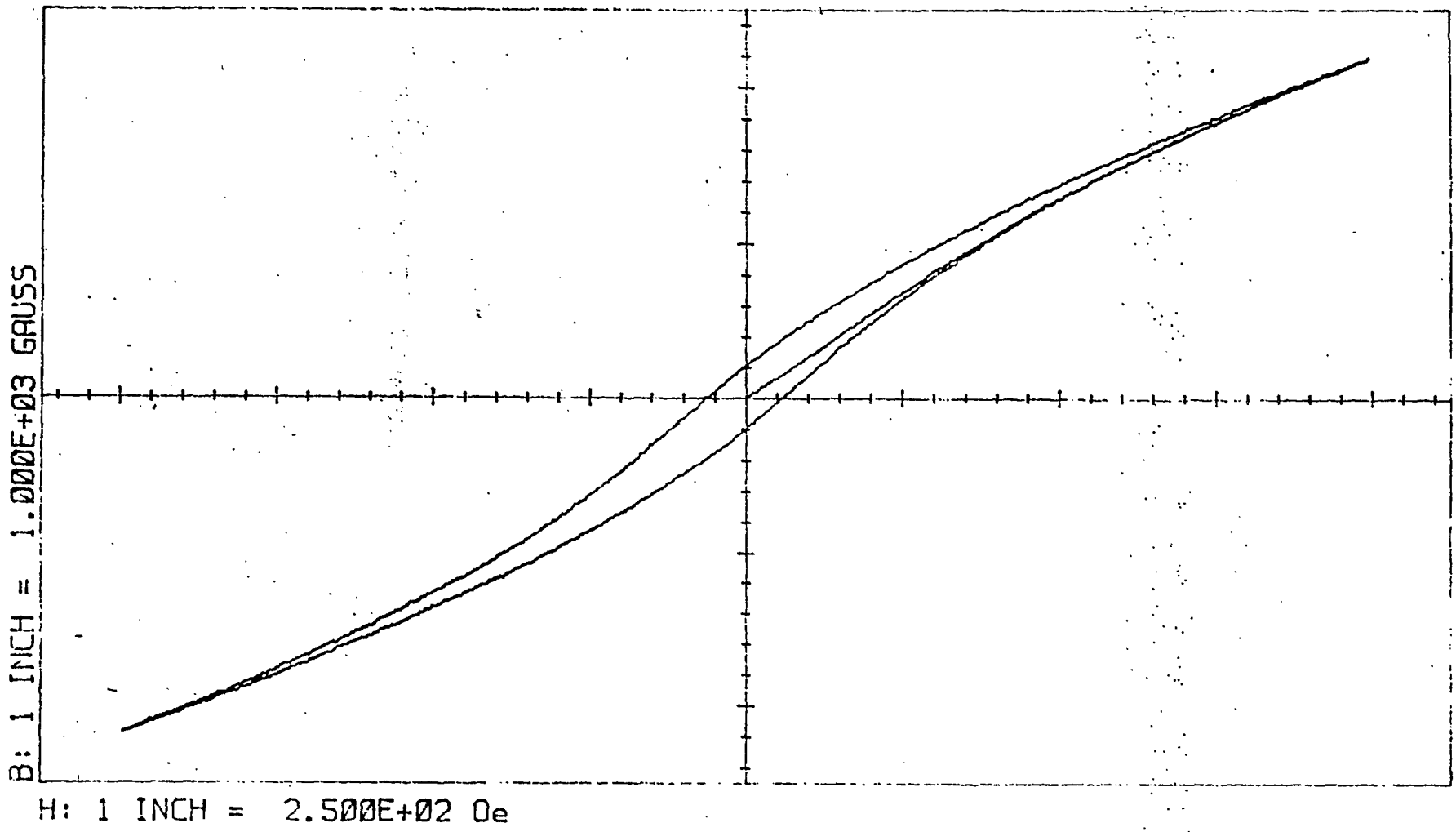

E96 POWDER
Hm= 9.985E+02 Oe
Bm= 2.183E+03 GAUSS
Hc= 6.050E+01 Oe
Br= 2.028E+02 GAUSS

BoHo= 2.943E+03 GAUSS-Oe
Ho= 2.600E+01 Oe
Bo= 1.132E+02 GAUSS
L-AREA= 2.772E+05 G-Oe
Mu @ Bm= 2.187E+00

Fig. 6 — Hysteresis loop of E-96 powder specimen

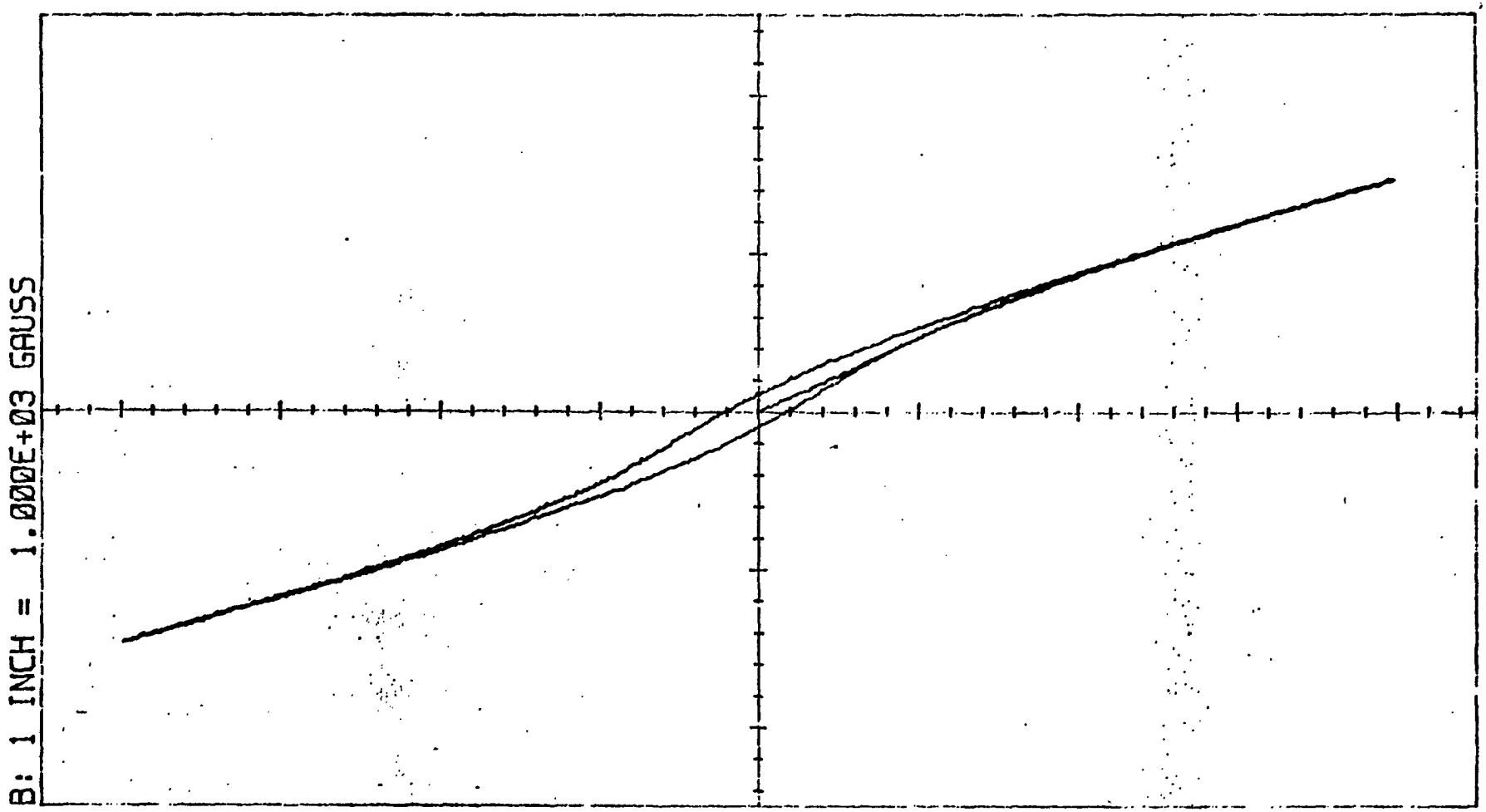

HOIST ROPE CORROSION PRODUCT

Hm= 9.990E+02 Oe
Bm= 1.462E+03 GAUSS
Hc= 4.725E+01 Oe
Br= 1.085E+02 GAUSS

BoHo= 1.297E+03 GAUSS-Oe
Ho= 2.750E+01 Oe
Bo= 4.716E+01 GAUSS
L-AREA= 9.694E+04 G-Oe
Mu @ Bm= 1.463E+00

Fig. 7 — Hysteresis loop of corrosion product powder specimen

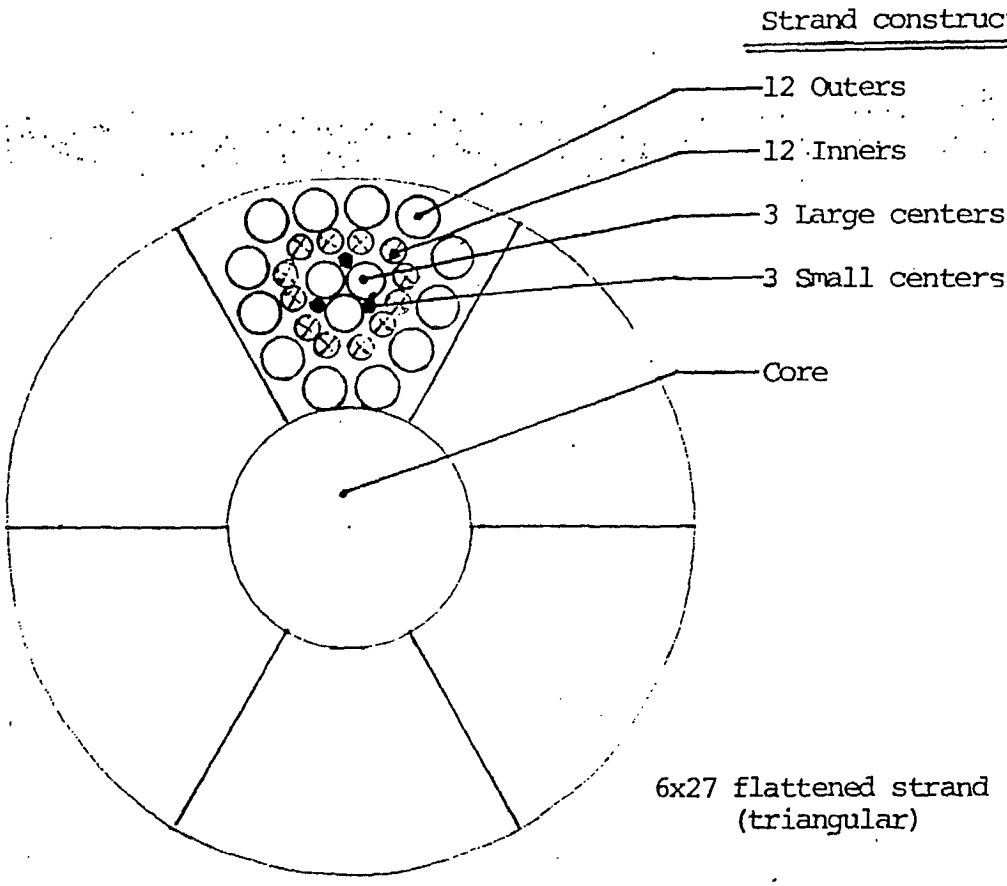

STRAND CONSTRUCTION	LMA (total)
12 Outers	62%
12 Inners	22%
3+3 Centers	16%

Loss of one outer wire = 0,86% LMA
Loss of one inner wire = 0,31% LMA

Fig. 8 — Construction of test-ropes

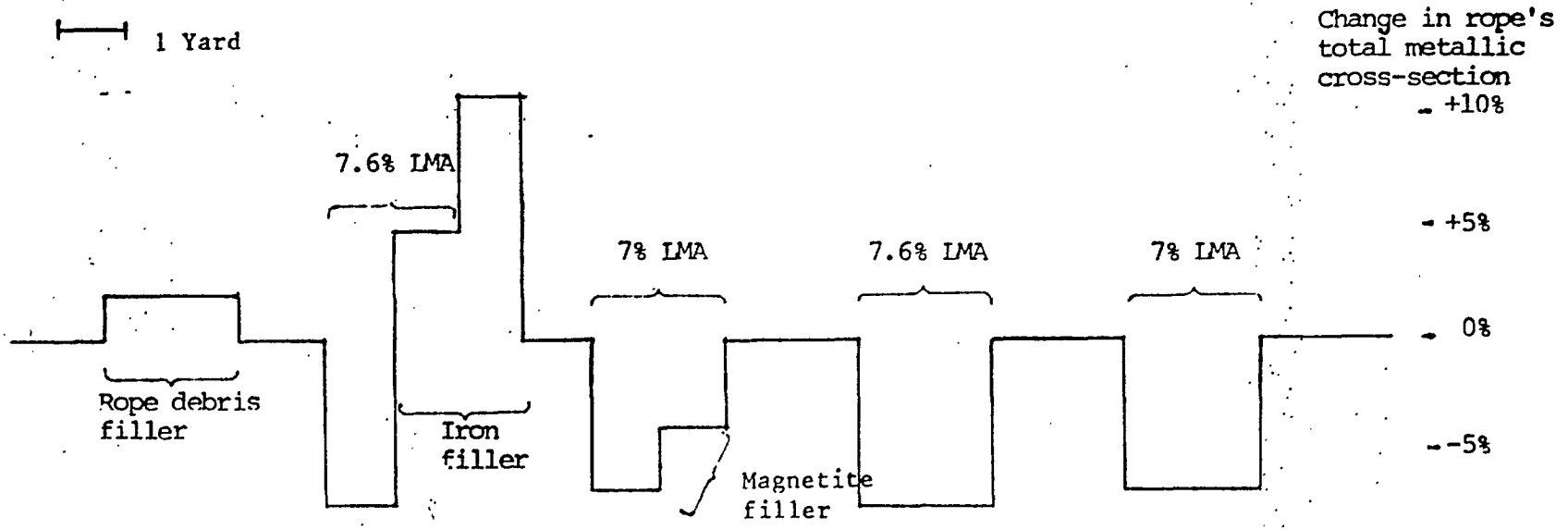

Fig. 9 — Test-rope A; schematic of theoretical defect-signal

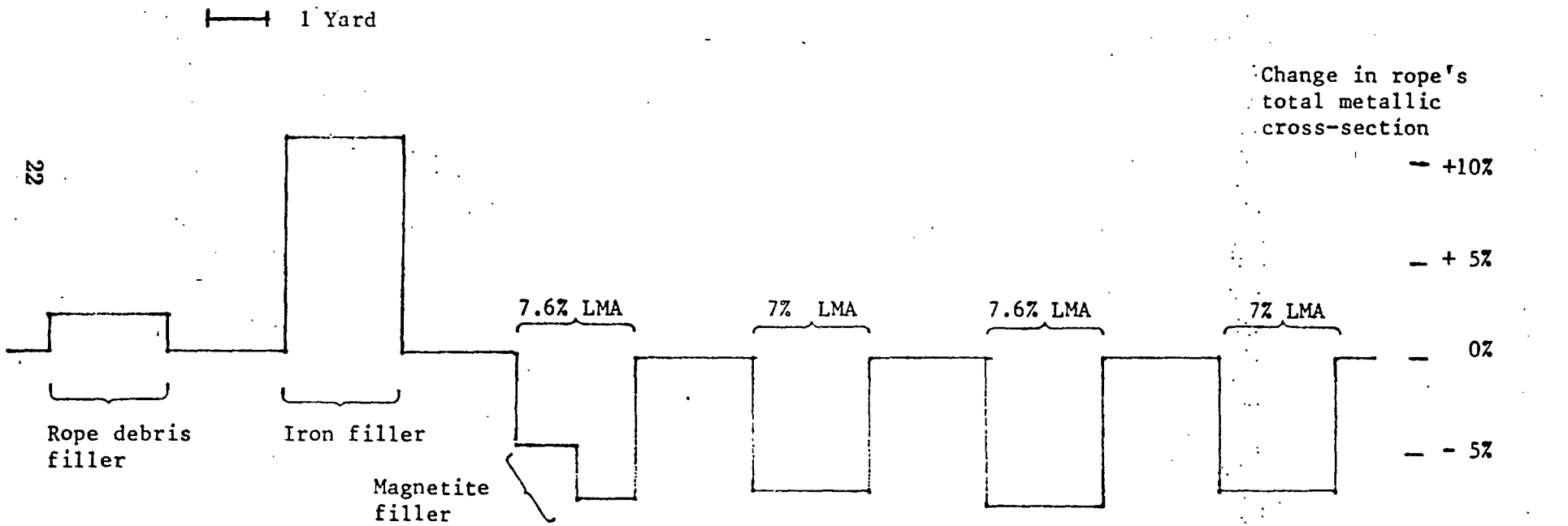

Fig. 10 — Test-rope B; schematic of theoretical defect-signal

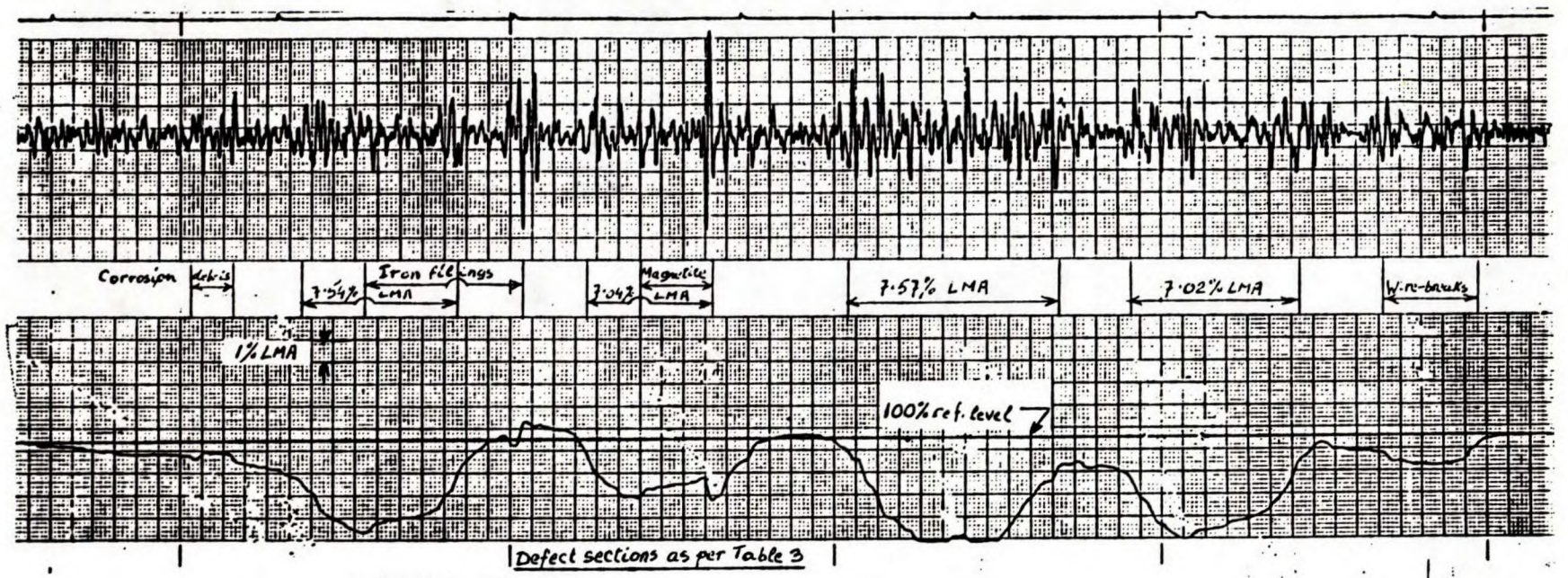

Fig. 11 — Test-rope A; Rotescograph's LMA chart-trace

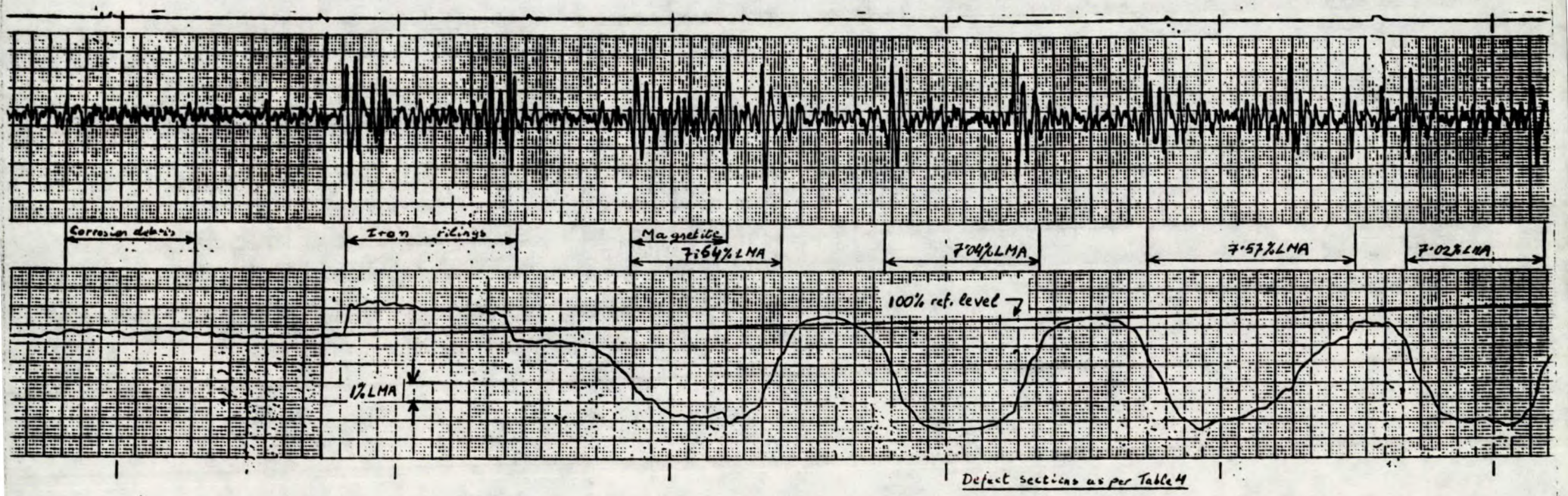

Fig. 12 — Test-rope B; Rotescograph's LMA chart-trace

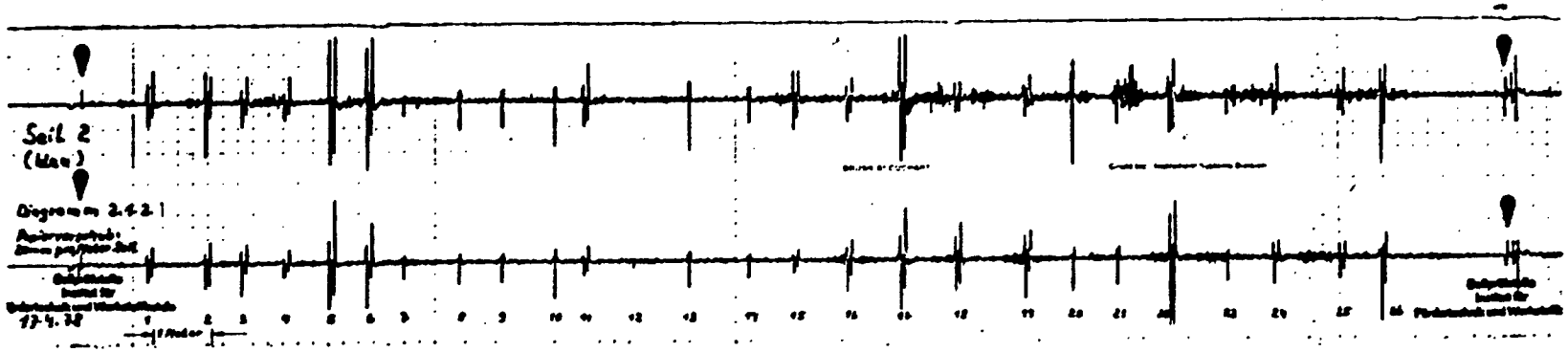

Fig.13 — Copy of WBK chart #2.1.2

Fig.14 — Copy of WBK chart #2.2.2

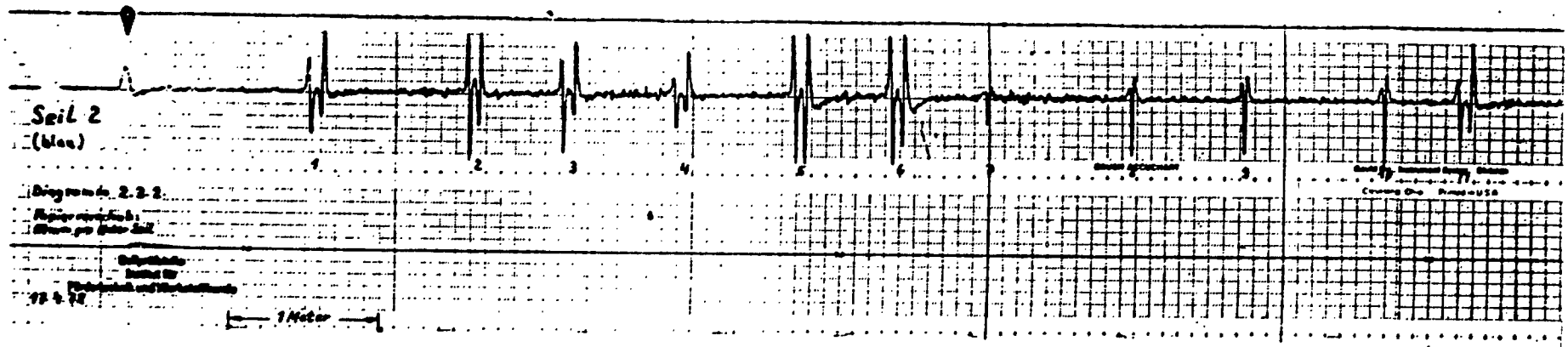

Fig.15 — Copy of WBK chart #2.3.2

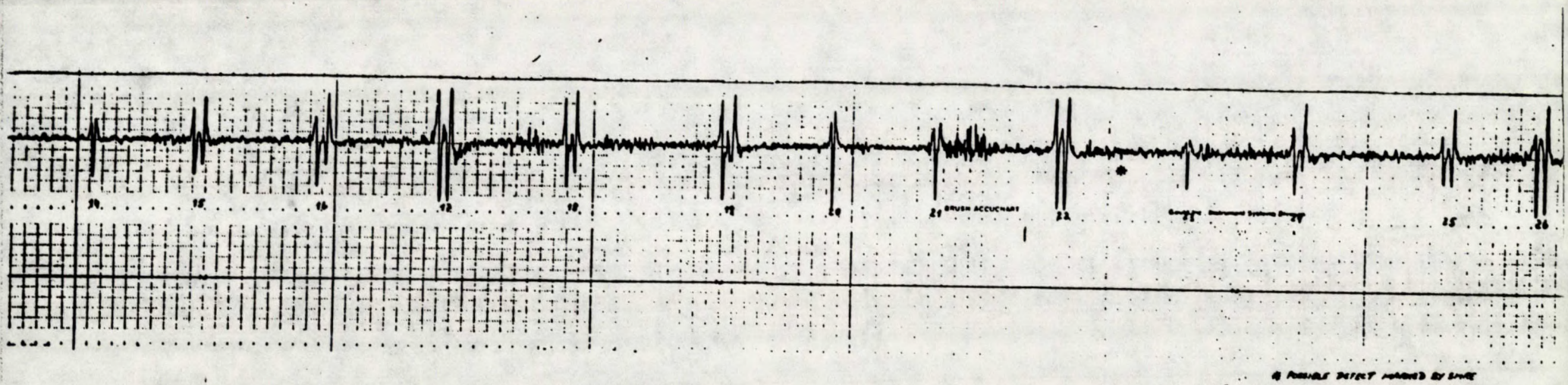

Fig.15a — Copy of WBK chart #2.3.2 (continued)

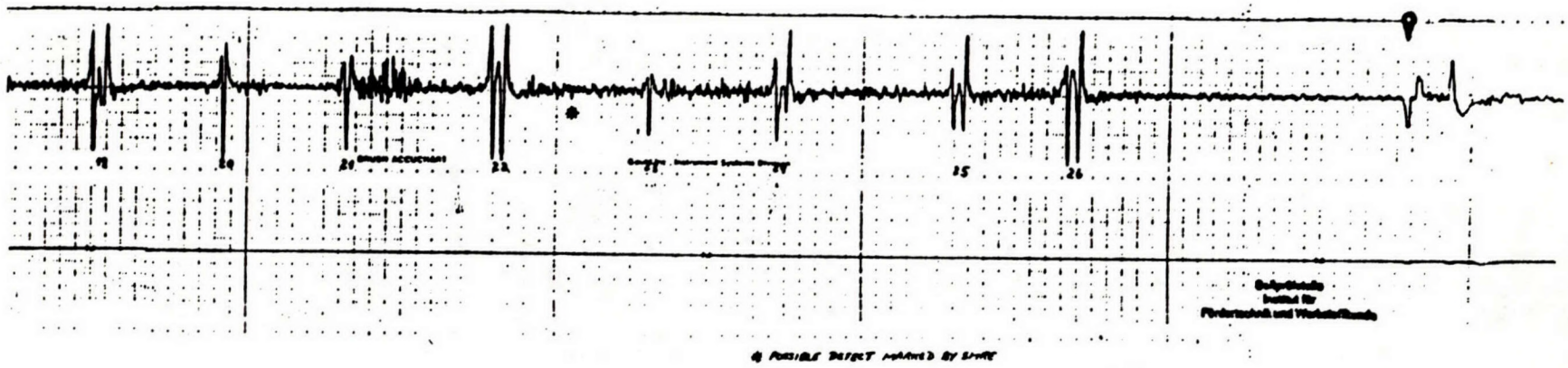

Fig.15b — Copy of WBK chart #2.3.2 (continued)